Supporting information

Experimental visualization of interstitialcy diffusion of Li ion in β-Li_2TiO_3

Keisuke Mukai,[1]* Masatomo Yashima,[2]* Keisuke Hibino,[2] Takayuki Terai[3]

[1] Institute of Advanced Energy, Kyoto University, Kyoto 611-0011, Japan

[2] Department of Chemistry, School of Science, Tokyo Institute of Technology, 2-12-1-W4-17, O-okayama, Meguro-ku, Tokyo, 152-8551, Japan

[3] Department of Nuclear Engineering and Management, School of Engineering, The University of Tokyo, 7-3-1 Hongo, Bunkyo-ku, Tokyo 113-8656, Japan

* Corresponding author: k-mukai@iae.kyoto-u.ac.jp (KM); yashima@cms.titech.ac.jp (MY).

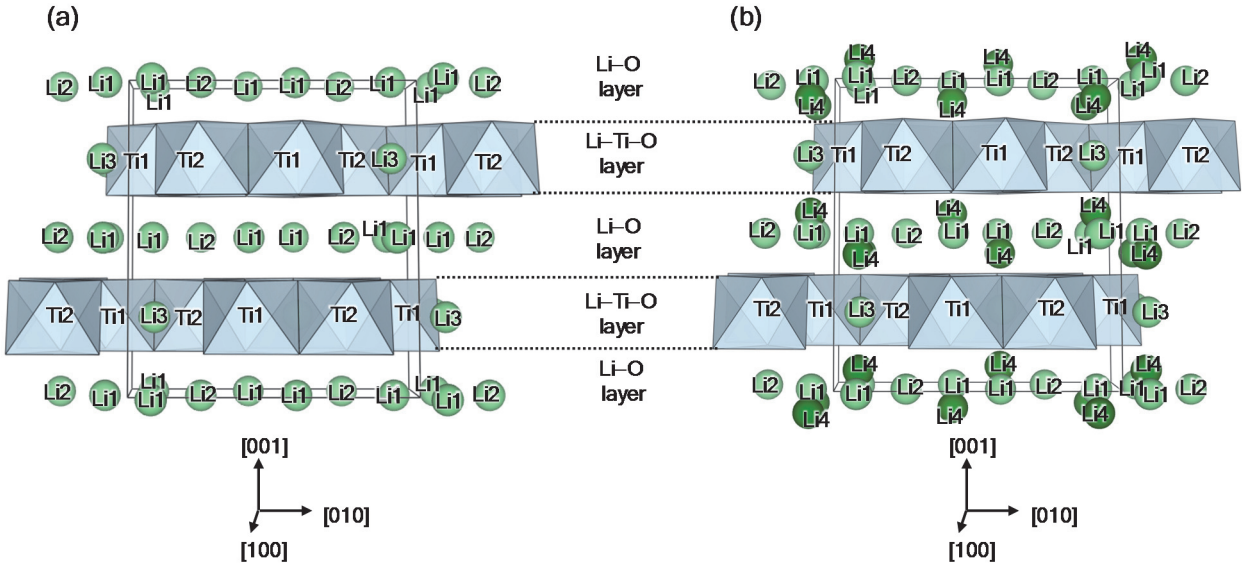

Figure S1. Refined crystal structures of β-$^7Li_2TiO_3$ for the TOF-ND data at RT based on the (a) conventional and (b) interstitial models. These figures were drawn with TiO_6 octahedra and Li cations. The light green and dark green spheres and blue octahedra represent Li atoms at the Li lattice sites Li*i* (*i* = 1, 2, and 3), Li atoms at interstitial Li4 site, and TiO_6, respectively.

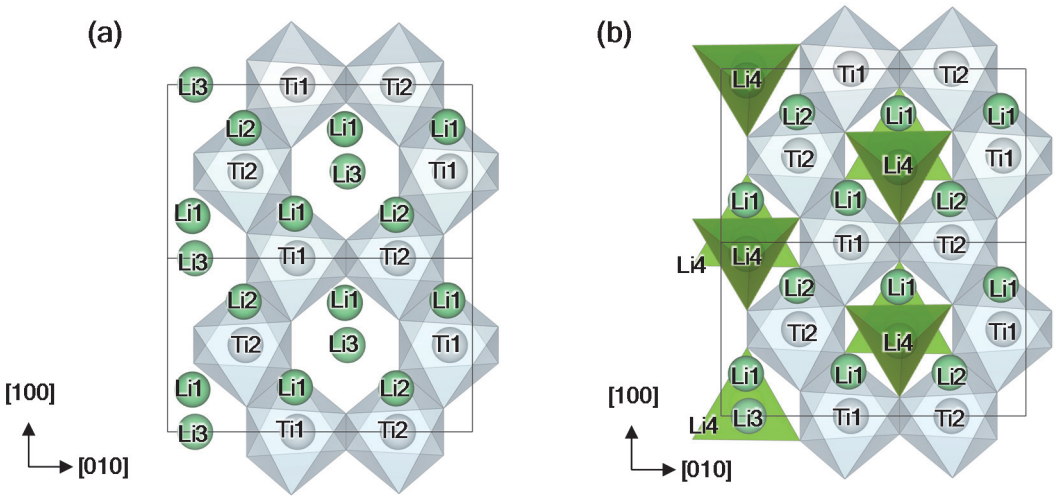

Figure S2. Refined crystal structures of β-$^{7}Li_2TiO_3$ for the TOF-ND data at RT projected along the [001] direction based on the (a) conventional and (b) interstitial models. The light green and grey spheres, blue octahedra, and dark green tetrahedra represent Li atoms at the Li lattice sites Li*i* (*i* = 1, 2 and 3), Ti atoms, TiO_6, and $Li4O_4$, respectively.

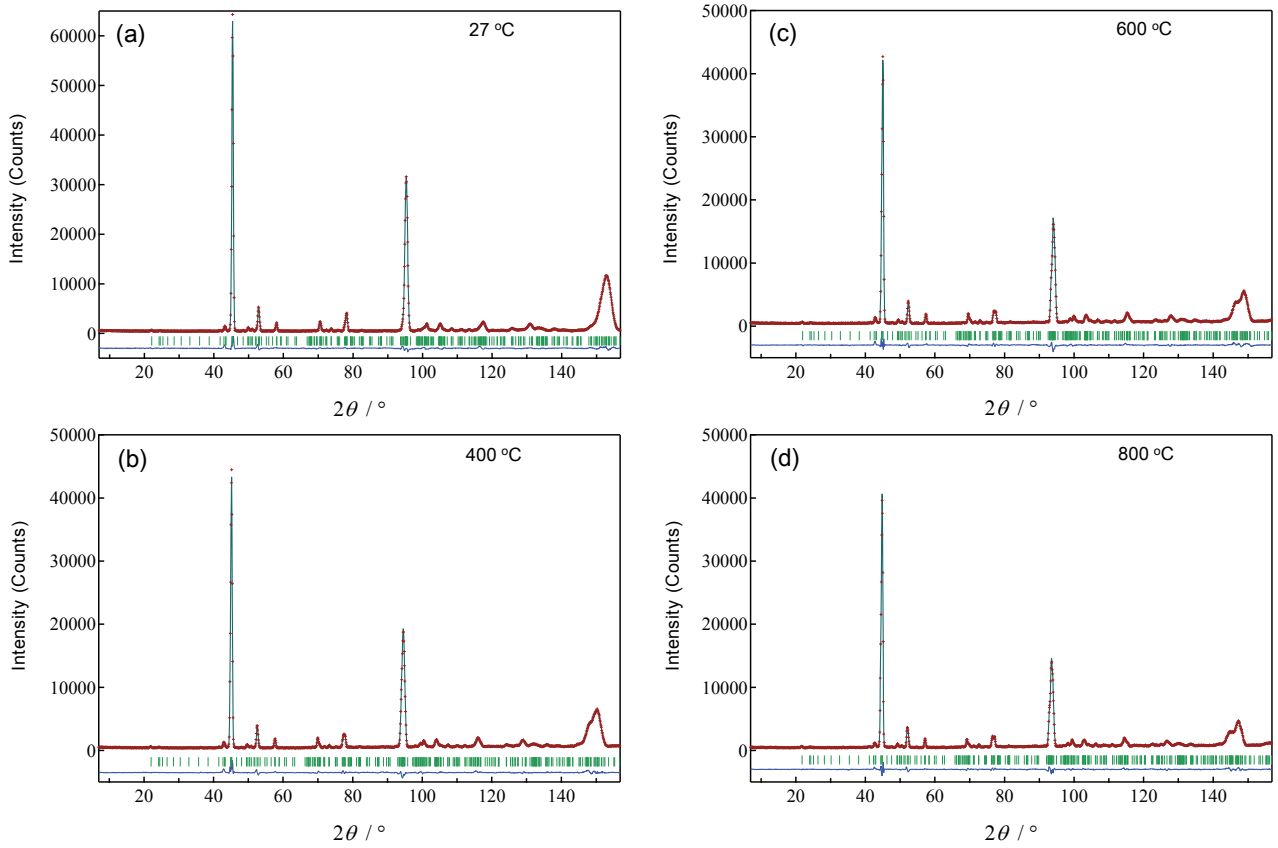

Figure S3. Rietveld patterns of the neutron powder diffraction data of β-$^{7}Li_2TiO_3$ measured *in situ* at (a) 27, (b) 400, (c) 600, and (d) 800 °C, which were plotted with respect to 2θ. The observed intensity I_{obs}, calculated intensity I_{calc}, intensity difference ($I_{obs} - I_{calc}$), and calculated Bragg peak positions are represented by red plus marks, a dark green solid line, blue line, and green tick marks, respectively. The refined crystal parameters and reliability factors (*R* factors) are listed in Tables S1b (27 °C), S4 (400 °C), S5 (600 °C), and S6 (800 °C).

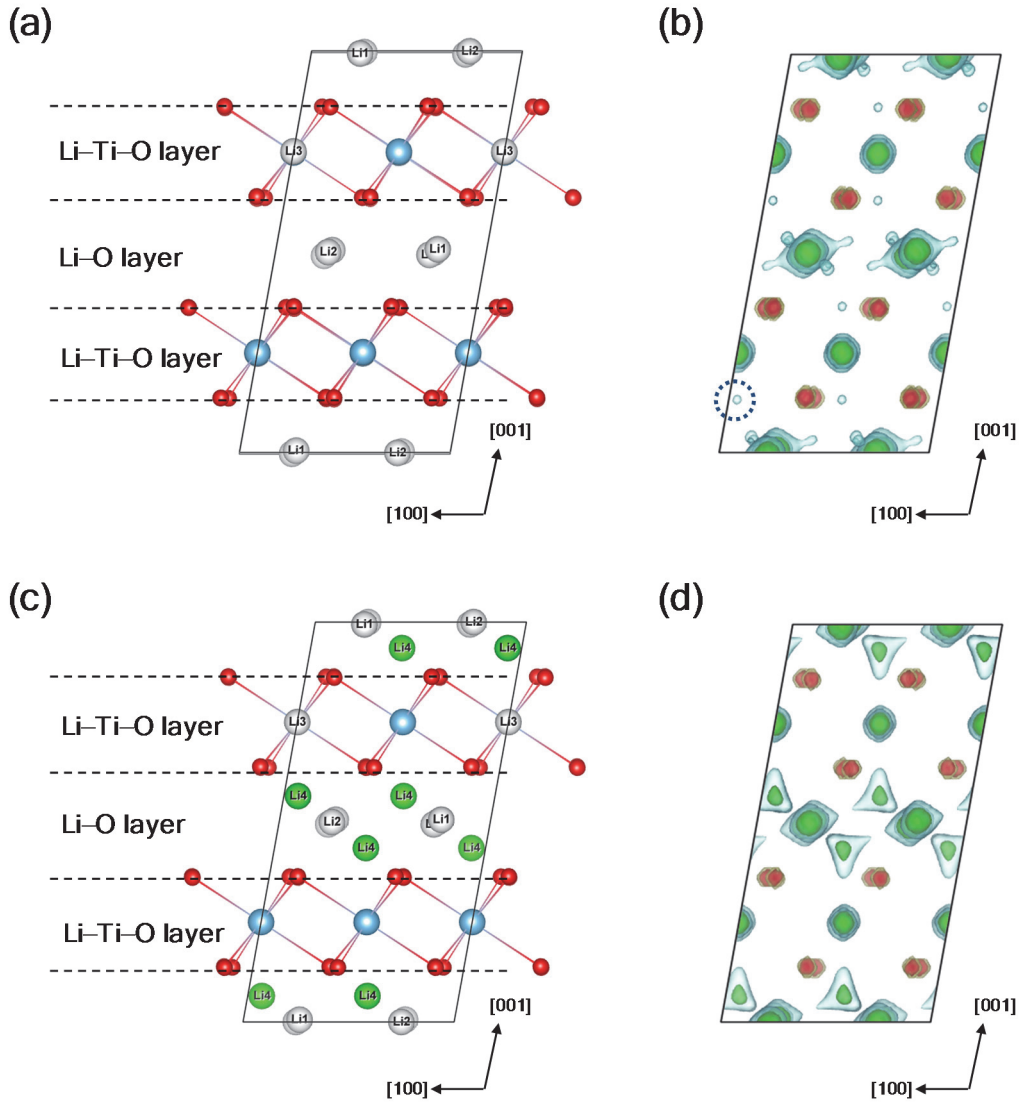

Figure S4. Refined crystal structure and MEM nuclear-density distribution of β-$^{7}Li_2TiO_3$, based on the conventional model without interstitial Li ions (a, b) and the interstitial model with the interstitial Li ion at the Li4 8*f* site (atomic coordinates: 0.9, 0.1, 0.1) (c, d). Rietveld and MEM analyses were performed using the neutron-diffraction data of β-$^{7}Li_2TiO_3$ measured at RT by HERMES. In panels a and c, the green, white, light blue, and red spheres represent Li4, Li*i* (*i* = 1, 2, and 3), Ti, and O atoms, respectively. Panels b and d show the green, light green, yellow and red isosurfaces of the nuclear densities at –1.0, –0.02, +0.02, and +1.0 fm Å^{-3}, respectively. In panel b, the dashed circle represents the nuclear density at the 0.9, 0.1, 0.1 position, suggesting an interstitial Li4 atom at the 8*f* site.

Table S1. Crystal parameters of β-$^7Li_2TiO_3$, which were refined by the Rietveld analysis of neutron powder diffraction data measured at RT.

(a) Anisotropic atomic displacement parameters of oxygen atoms refined using the neutron diffraction data measured by iMATERIA (interstitial model). The atomic coordinates, lattice parameters, reliability factors are listed in Table 1.

Atom label	U_{11} Å^2	U_{22} Å^2	U_{33} Å^2	U_{12} Å^2	U_{13} Å^2	U_{23} Å^2
O1	0.0046(3)	0.0053(2)	0.0060(3)	–0.0020(2)	–0.0014(2)	–0.0014(2)
O2	0.0058(2)	0.0042(2)	0.0060(3)	0.0016(2)	0.0010(2)	0.0001(3)
O3	0.0044(2)	0.0055(2)	0.0060(3)	0.0018(2)	–0.0007(2)	0.0017(2)

(b) Crystal parameters of β-$^7Li_2TiO_3$, which were refined by the Rietveld analysis of neutron powder diffraction data measured by HERMES at 27 °C (interstitial model).

Atom label	Occupancy	x	y	z	U_{iso} Å^2
Li1	0.971(6)	0.234(3)	0.0854(16)	0.0059(12)	0.0105(4)
Li2	0.971(6)	1/4	1/4	1/2	0.0105(4)
Li3	0.956(6)	0	0.096(3)	1/4	0.0074(2)
Li4	0.066(11)	0.933	0.085	0.065	0.0098(3)
Ti1	1	0	0.4186(18)	1/4	0.00150(5)
Ti2	1	0	0.7510(18)	1/4	0.00147(5)
O1	1	0.1367(8)	0.2634(6)	0.1388(6)	0.00194(6)
O2	1	0.0976(8)	0.5857(6)	0.1366(4)	0.00197(7)
O3	1	0.1343(7)	0.9073(6)	0.1360(5)	0.00198(7)
crystal system: monoclinic, space group: *C*2/*c* lattice parameters*:* a = 5.0620(2) Å, b = 8.7861(4) Å, c = 9.7560(4) Å, β = 100.239(5)°; lattice volume: 426.99(3) Å^3					
reliability factors in Rietveld analysis: R_{wp} = 6.43%, R_I = 1.41%, R_F = 0.58%, goodness-of-fit (GoF) = 2.41					
linear constrains	U_{iso}(Li1) = U_{iso}(Li2) = 1.429U_{iso}(Li3) = 1.077U_{iso}(Li4) = 7U_{iso}(Ti1) = 7U_{iso}(Ti2) = 5.426U_{iso}(O1) = 5.344U_{iso}(O2) = 5.303U_{iso}(O3) and g(Li1) = g(Li2) = 1.015g(Li3) = 1.004 – 0.502g(Li4).				

(c) Crystal parameters and BVSs of β-$^7Li_2TiO_3$, which were refined by the Rietveld analysis of neutron powder diffraction data measured by iMATERIA at RT (conventional model).

Atom label	Wyckoff site	occupancy	x	y	z	U_{iso}[a] or U_{eq}[b] Å^2	BVS vu
Li1	8*f*	1	0.2425(3)	0.0822(2)	–0.0003(2)	0.01045(3)[a]	0.985(2)
Li2	4*d*	1	1/4	1/4	1/2	0.01078(6)[a]	0.980(1)
Li3	4*e*	0.975(5)	0	0.0937(2)	1/4	0.00478(3)[a]	1.081(2)
Ti1	4*e*	1	0	0.4288(5)	1/4	0.00296(2)[a]	3.854(5)
Ti2	4*e*	1	0	0.75721(14)	1/4	0.00285(2)[a]	4.117(3)
O1	8*f*	1	0.14283(10)	0.25913(6)	0.13773(7)	0.00531(11)[b]	1.923(6)
O2	8*f*	1	0.10479(10)	0.58543(6)	0.13589(5)	0.00534(10)[b]	2.044(8)
O3	8*f*	1	0.13547(10)	0.90573(5)	0.13519(5)	0.00551(10)[b]	2.034(6)

crystal system: monoclinic, space group: *C*2/*c*

lattice parameters: a = 5.066611(16) Å, b = 8.78583(3) Å, c = 9.74892(2) Å, β = 100.1045(3)°; lattice volume: 427.235(3) Å^3

reliability factors in Rietveld analysis: R_{wp} = 10.574%, R_p = 7.992 %, R_e = 2.565%, R_I = 7.045%, R_F = 4.737%

[a] U_{iso}: Isotropic atomic displacement parameter (ADP) of Li and Ti atoms.

[b] U_{eq}: Equivalent isotropic ADP. Refined anisotropic ADPs U_{ij} of oxygen atoms are listed below.

Atom label	U_{11} Å^2	U_{22} Å^2	U_{33} Å^2	U_{12} Å^2	U_{13} Å^2	U_{23} Å^2
O1	0.0046(3)	0.0053(2)	0.0060(3)	–0.0020(2)	–0.0014(2)	–0.0014(2)
O2	0.0058(2)	0.0042(2)	0.0060(3)	0.0016(2)	0.0010(2)	0.0001(3)
O3	0.0044(2)	0.0055(2)	0.0060(3)	0.0018(2)	–0.0007(2)	0.0017(2)

(d) Crystal parameters of β-$^7Li_2TiO_3$, which were refined by the Rietveld analysis of neutron powder diffraction data measured by HERMES at RT (conventional model).

Atom label	Occupancy	x	y	z	U_{iso} Å^2
Li1	1	0.232(2)	0.0862(15)	0.0063(11)	0.0105(4)
Li2	1	1/4	1/4	1/2	0.00105(4)
Li3	1	0	0.094(2)	1/4	0.0074(2)
Ti1	1	0	0.4172(15)	1/4	0.00150(5)
Ti2	1	0	0.7484(15)	1/4	0.00147(5)
O1	1	0.1367(7)	0.2638(5)	0.1385(6)	0.00194(6)
O2	1	0.0976(7)	0.5862(5)	0.1366(4)	0.00197(7)
O3	1	0.1343(7)	0.9077(5)	0.1362(4)	0.00198(7)

crystal system: monoclinic, space group: *C*2/*c*

lattice parameters: a = 5.0620(2) Å, b = 8.7861(4) Å, c = 9.7560(4) Å, β = 100.239(5)°; lattice volume: 426.99(3) Å^3

reliability factors in Rietveld analysis: R_{wp} = 6.51%, R_I = 1.65, R_F = 0.73%, goodness-of-fit (GoF) = 2.44

constrains: U_{iso}(Li1) = U_{iso}(Li2) = 1.429U_{iso} (Li3) = 1.077U_{iso}(Li4) = 7U_{iso}(Ti1) =7U_{iso}(Ti2) = 5.426U_{iso}(O1) = 5.344U_{iso}(O2) = 5.303U_{iso}(O3).

Table S2. Crystallographic parameters and energy difference between the conventional and interstitial models calculated by density functional theory computations. The lattice parameters were obtained by allowing atomic positions and lattice parameters to change in the relaxation. The obtained lattice parameters and the atomic positions refined using TOF-ND data at RT with iMateria (Table 1) were used as an initial crystal structure. The local structure surrounding the Li4 atom after relaxation is displayed in Figure 2c and Figure S5b. Numbers in the parentheses show the differences between the relaxed atomic positions by the DFT calculations and positions refined using the TOF-ND data taken at RT with iMATERIA. A 2 × 1 × 1 supercell with stoichiometric composition was used for the calculation. The interstitial model contained one negatively charged vacancy at Li3 site and a distantly positioned Li^+ ion at the Li4 site, while the octahedral Li sites were fully occupied in the conventional model. The optimized lattice parameters *a*, *b*, and *c* agreed with the experimental ones. The atomic coordinates relaxed in DFT calculations agreed well with those refined by the Rietveld analysis of neutron diffraction data taken with the iMATERIA at RT. The difference in total energy between the conventional and interstitial models was negligibly small ($E_{int.} - E_{conv.}$ = 18.3 m eV).

atom label	*x*	*y*	*z*	BVS vu
Li4	0.934 (0.001)	0.092 (0.007)	0.071 (0.006)	1.18
lattice parameter: a = 5.09 Å, b = 8.83 Å, c = 9.80 Å, β = 100.25°; lattice volume: 435.30 Å^3				
$E_{int.} - E_{conv.}$	18.3 meV / atom			

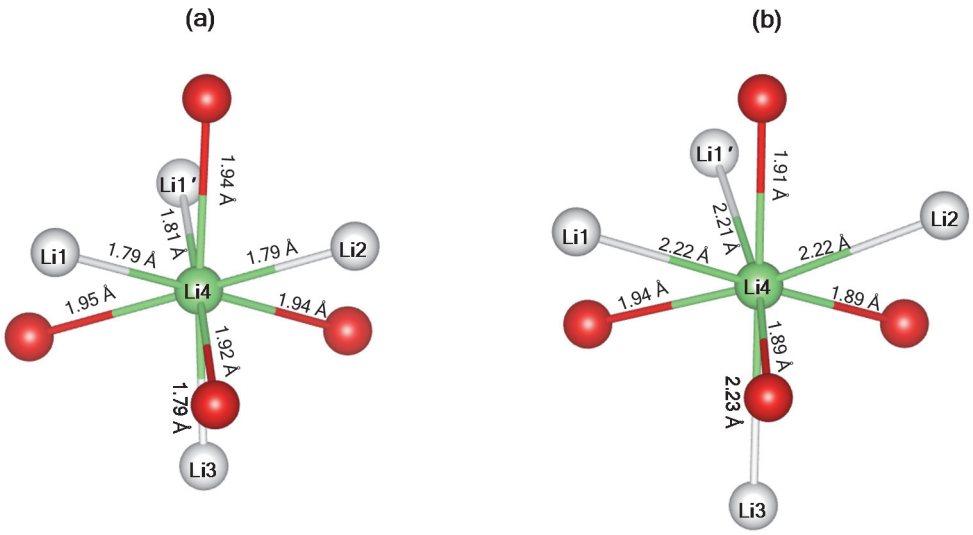

Figure S5. Local configuration surrounding an interstitial Li4 atom (a) before and (b) after relaxation of atomic positions by DFT calculation where the cell parameters were fixed during the relaxation to the values in the DFT optimization of both cell and positional parameters. The white, green, and red spheres stand for Li atom at the octahedral site, interstitial Li atom at the Li4 site, and O atoms, respectively. The atomic positions and displacements are listed in Table S3. The calculated interatomic distances in panel a was slightly longer than those from the iMATERIA neutron data at RT (Figure 2a), because the cell volume in the DFT calculation was a little larger than the experimental data (Table 1 and Table S2). The relaxed Li–Li interatomic distances were longer than the initial ones, while the Li–O distances were almost unchanged. While the displacements of interstitial Li4 and oxygen atoms were smaller than 0.1 Å, Li atoms at the Li*i* (*i* = 1, 1′, 2, and 3) lattice sites were largely displaced by Li–Li repulsion, which resulted in longer Li4–Li*i* distances in the optimized structure.

Table S3. Atomic coordinates and displacements of Li and O atoms obtained by DFT calculations. Left and right panels in Figure S5 show the initial and final states, respectively, in the structural optimisation.

Atom label	Initial atomic position	Optimized atomic position	Displacement Å
Li1	(0.372, 0.418, 0.500)	(0.384, 0.381, 0.515)	0.373
Li1′	(0.128, 0.582, 0.500)	(0.096, 0.563, 0.513)	0.406
Li2	(0.375, 0.750, 0.500)	(0.400, 0.788, 0.527)	0.475
Li3	(0.250, 0.591, 0.250)	(0.242, 0.586, 0.198)	0.504
Li4	(0.284, 0.585, 0.435)	(0.283, 0.592, 0.430)	0.083
Oxygen	(0.182, 0.406, 0.365)	(0.182, 0.411, 0.367)	0.053
	(0.318, 0.594, 0.635)	(0.322, 0.595, 0.627)	0.096
	(0.447, 0.586, 0.364)	(0.445, 0.585, 0.361)	0.040
	(0.179, 0.759, 0.363)	(0.180, 0.763, 0.360)	0.044

Table S4. Crystal parameters of β-$^7Li_2TiO_3$ at 400 °C, which were refined by the Rietveld analysis of neutron powder diffraction data *in situ* measured by HERMES.

Atom label	Occupancy	*x*	*y*	*z*	U_{iso} Å^2
Li1	0.973(6)	0.236(3)	0.089(2)	0.0024(14)	0.0236(3)
Li2	0.973(6)	1/4	1/4	1/2	0.0236(3)
Li3	0.939(6)	0	0.095(3)	1/4	0.0175(2)
Li4	0.072(12)	0.933	0.085	0.065	0.0230(3)
Ti1	1	0	0.4234(14)	1/4	0.00575(7)
Ti2	1	0	0.7515(15)	1/4	0.0575(7)
O1	1	0.1352(10)	0.2665(5)	0.1395(7)	0.00805(10)
O2	1	0.0988(8)	0.5879(6)	0.1374(5)	0.00805(10)
O3	1	0.1368(8)	0.9085(6)	0.1362(5)	0.0805(10)
space group: *C*2/*c*					
lattice parameters: a = 5.0942(2) Å, b = 8.842(4) Å, c = 9.8441(3) Å, β = 100.266(4)°; lattice volume: V = 436.30(3) Å^3					
reliability factors in Rietveld analysis: R_{wp} = 6.33%, R_I = 2.53, R_F = 1.15%, goodness-of-fit (GoF) = 2.11					
linear constrains	U_{iso}(Li1) = U_{iso}(Li2) = 1.344U_{iso}(Li3) = 1.025U_{iso}(Li4) = 4.100U_{iso}(Ti1) =4.100U_{iso}(Ti2) = 2.887U_{iso}(O1) = 2.887U_{iso}(O2) = 2.887U_{iso}(O3) and g(Li1) = g(Li2) = 1.036g(Li3) = 1.009 – 0.505g(Li4).				

Table S5. Crystal parameters of β-$^7Li_2TiO_3$ at 600 °C, which were refined by the Rietveld analysis of neutron powder diffraction data *in situ* measured by HERMES.

Atom label	Occupancy	*x*	*y*	*z*	U_{iso} Å^2
Li1	0.972(7)	0.238(3)	0.090(3)	0.0003(16)	0.0334(5)
Li2	0.972(7)	1/4	1/4	1/2	0.0334(5)
Li3	0.923(6)	0	0.095(3)	1/4	0.0312(5)
Li4	0.080(13)	0.933	0.085	0.065	0.0326(5)
Ti1	1	0	0.4246(15)	1/4	0.00918(15)
Ti2	1	0	0.7535(15)	1/4	0.00918(15)
O1	1	0.1354(11)	0.2679(6)	0.1394(7)	0.0131(2)
O2	1	0.0993(9)	0.5881(6)	0.1376(5)	0.0131(2)
O3	1	0.1374(8)	0.9092(7)	0.1366(6)	0.0131(2)
space group: *C*2/*c*					
lattice parameters: a = 5.1130(2) Å, b = 8.8772(4) Å, c = 9.8925(3) Å, β = 100.254(5)°; lattice volume: V = 441.84(3) Å^3					
reliability actors in Rietveld analysis: R_{wp} = 6.35%, R_I = 2.06, R_F = 1.12%, goodness-of-fit (GoF) = 2.14					
linear constrains	U_{iso}(Li1) = U_{iso}(Li2) = 1.071U_{iso}(Li3) = 1.025U_{iso}(Li4) = 3.64U_{iso}(Ti1) =3.64U_{iso}(Ti2) = 2.545U_{iso}(O1) = 2.545U_{iso}(O2) = 2.545U_{iso}(O3) and g(Li1) = g(Li2) = 1.054g(Li3) = 1.012 – 0.506g(Li4).				

Table S6. Crystal parameters of β-$^7Li_2TiO_3$ at 800 °C, which were refined by the Rietveld analysis of neutron powder diffraction data *in situ* measured by HERMES.

Atom label	Occupancy	*x*	*y*	*z*	U_{iso} Å^2
Li1	0.972(6)	0.232(3)	0.087(3)	0.0017(14)	0.0448(2)
Li2	0.972(6)	1/4	1/4	1/2	0.0448(2)
Li3	0.911(5)	0	0.100(3)	1/4	0.0384(2)
Li4	0.086(11)	–0.067	0.085	0.065	0.0448(2)
Ti1	1	0	0.4247(14)	1/4	0.01281(7)
Ti2	1	0	0.7522(14)	1/4	0.01281(7)
O1	1	0.1360(10)	0.2675(5)	0.1395(7)	0.02178(12)
O2	1	0.0985(8)	0.5873(6)	0.1388(5)	0.02178(12)
O3	1	0.1378(8)	0.9087(7)	0.1353(5)	0.02178(12)
space group: *C*2/*c*					
lattice parameters: a = 5.12847(18) Å, b = 8.90382(32) Å, c = 9.9328(39) Å, β = 100.2539(5)°; lattice volume: 446.31(3) Å^3					
reliability factors in Rietveld analysis: R_{wp} = 5.463%, R_I = 1.02%, R_F = 0.73%, goodness-of-fit (GoF) = 1.80					
linear constrains	U_{iso}(Li1) = U_{iso}(Li2) = 1.167U_{iso}(Li3) = U_{iso}(Li4) = 3.5U_{iso}(Ti1) = 3.5U_{iso}(Ti2) = 2.059U_{iso}(O1) = 2.059U_{iso}(O2) = 2.059U_{iso}(O3), g(Li1) = g(Li2) = 1.067g(Li3) = 1.016 – 0.508g(Li4).				

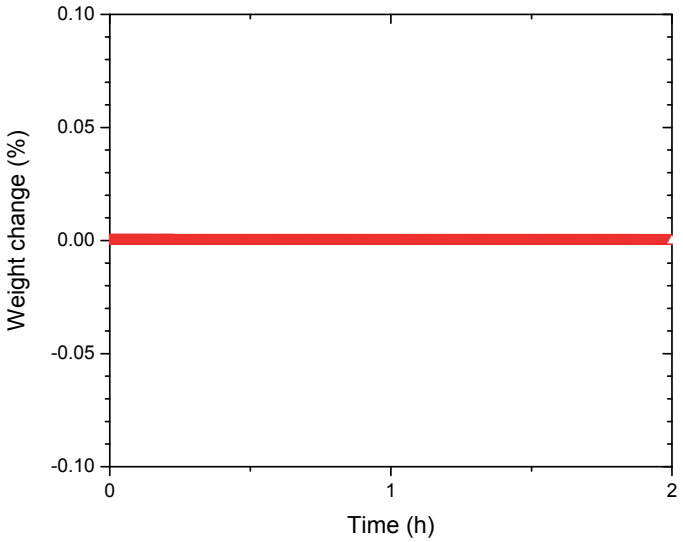

Figure S6. Results of the thermogravimetric measurement of β-Li_2TiO_3 powder at 800 °C in air. A stoichiometric β-Li_2TiO_3 specimen (initial weight: 72.17 mg) was heated at a heating rate of 15 ^oC min^{-1}. Thermogravimetric measurement started 1 h after the target temperature of 800 ^oC was reached. Weight changes at 800 °C in air were negligibly small**.**

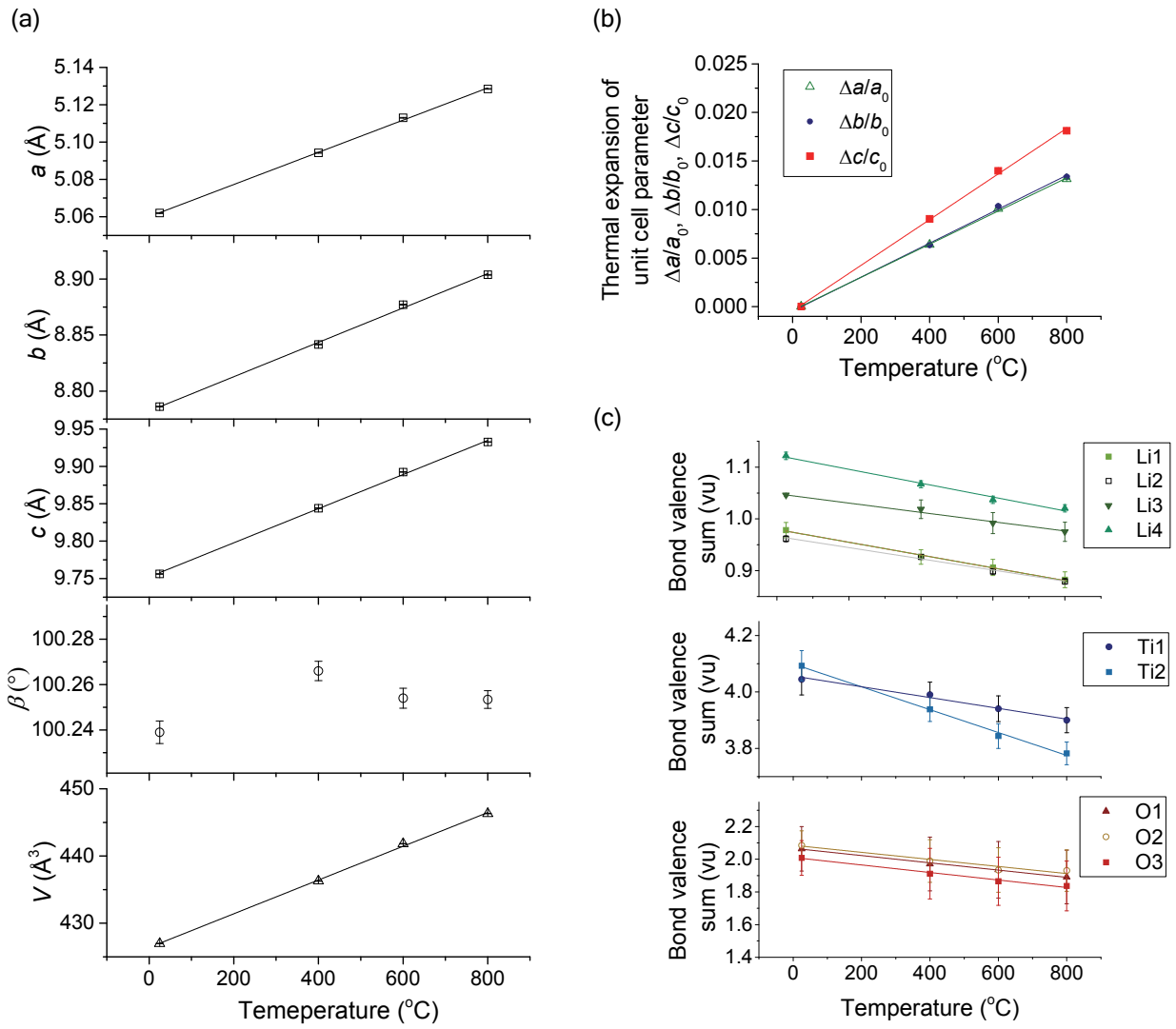

Figure S7. (**a**) Temperature dependence of the lattice parameters *a*, *b*, *c* and *β*, and lattice volume *V*, (**b**) thermal expansion of unit cell parameters, and (**c**) bond valence sum (BVS) of the crystal structure refined using the neutron diffraction data measured *in situ* with HERMES diffractometer at 27, 400, 600, and 800 °C. The BVS was calculated using the bond-valence parameters after Brown et al.[1] Thermal expansions of the unit cell parameters are defined as $\Delta a/a_0 \equiv [a(T) - a(27)]/a(27)$, $\Delta b/b_0 \equiv [b(T) - b(27)]/b(27)$, and $\Delta c/c_0 \equiv [c(T) - c(27)]/c(27)$ where $a(T)$, $b(T)$, and $c(T)$ are the lattice parameters *a*, *b*, and *c* at a temperature *T* (°C), respectively. The average thermal expansion coefficients along *a*, *b*, and *c* axes between 27 and 800 °C, defined as $\alpha_a \equiv [a(800) - a(27)]/a(27)/773$, $\alpha_b \equiv [b(800) - b(27)]/b(27)/773$, and $\alpha_c \equiv [c(800) - c(27)]/c(27)/773$. The α_a, α_b, and α_c were estimated to be $1.699(7) \times 10^{-5}$, $1.733(7) \times 10^{-5}$, and $2.344(7) \times 10^{-5}$ K^{-1}, respectively. α_c was 1.380(7) and 1.352(7) times higher than α_a and α_b, respectively, indicating the anisotropic thermal expansion of β-$^7Li_2TiO_3$. The average linear thermal expansion coefficient $\bar{\alpha}$ (K^{-1}) between 27 and 800 °C was defined as $\bar{\alpha} \equiv [V(800)^{1/3} - V(27)^{1/3}] / V(800)^{1/3} / 773$ where $V(T)$ is the lattice volume at *T* (°C). α of β-$^7Li_2TiO_3$ was $1.923(4) \times 10^{-5}$ K^{-1} and larger than that of the $LiNi_{0.33}Mn_{0.33}Co_{0.33}O_2$ cathode of Li-ion batteries ($1.2–1.3 \times 10^{-5}$ K^{-1} in the temperature range of 50–400 °C).[2] BVS decreased with an increase in temperature due to thermal expansion of the interatomic distance.

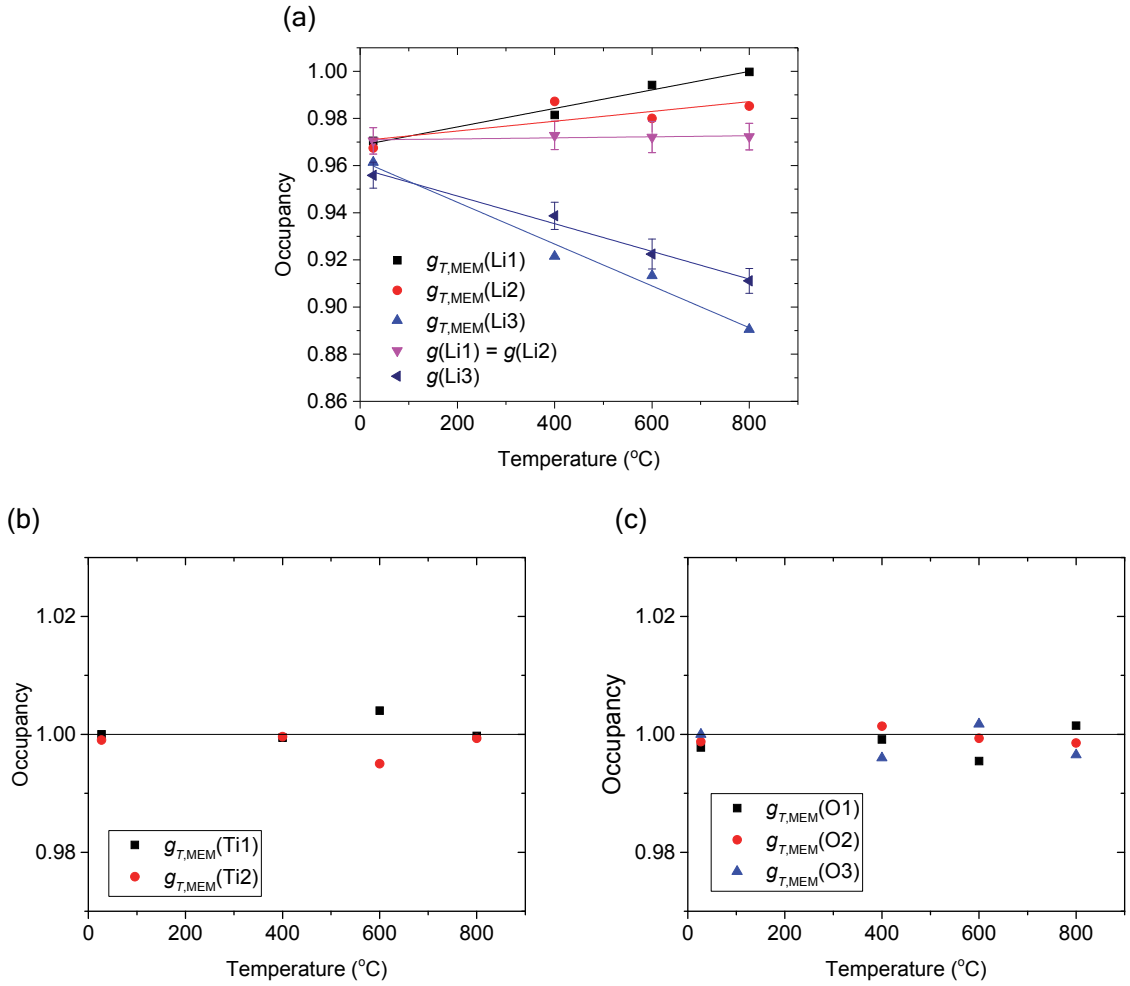

Figure S8. (**a**)–(**c**) Comparison between the occupancy factors obtained by Rietveld analyses and numbers of Li, Ti, and O atoms around each atomic site estimated using MEM nuclear-density distribution from the HERMES neutron data. Comparison of the occupancy factors at the Li4 site is shown in Figure 3a. g(Lii), g(Tij), and g(Ok) represent the refined occupancies at the Lii, Tij, and Ok sites, respectively, where i = 1, 2, 3, and 4, j = 1 and 2, and k = 1, 2, and 3. $g_{T,\mathrm{MEM}}$(Lii), $g_{T,\mathrm{MEM}}$(Tij), and $g_{T,\mathrm{MEM}}$(Ok) stand for the numbers of Li, Ti, and O atoms, respectively, which were calculated using the MEM nuclear-density distribution, which are defined as $g_{T,\mathrm{MEM}}(\mathrm{Li}i) \equiv g(\mathrm{Li1})I_{T,\mathrm{Li}i}/I_{27,\mathrm{Li1}}$, $g_{T,\mathrm{MEM}}(\mathrm{Ti}j) \equiv g(\mathrm{Ti1})I_{T,\mathrm{Ti}j}/I_{27,\mathrm{Ti1}}$, and $g_{T,\mathrm{MEM}}(\mathrm{O}k) \equiv g(\mathrm{O3})I_{T,\mathrm{O}k}/I_{27,\mathrm{O3}}$ where $I_{T,\mathrm{Li}i}$, $I_{T,\mathrm{Ti}j}$, and $I_{T,\mathrm{O}k}$ are the integrated values of neutron scattering length density around Lii, Tij, and Ok sites, respectively, at a temperature T (°C). It is noted that the occupancy factors at the Tij and Ok sites were fixed at 1 at all the temperatures as represented in Table1 and Table S1b, S4, S5, and S6. The numbers of Li, Ti, and O atoms estimated using MEM nuclear densities agreed with the refined occupancies in the Rietveld analyses. In panel a, the occupancy factors have the relation, g(Li1) = g(Li2). In panel b, the horizontal line denotes the occupancy factors of unity, g(Ti1) = g(Ti2) = 1. In panel c, the horizontal line denotes the occupancy factors of unity, g(O1) = g(O2) = g(O3) = 1.

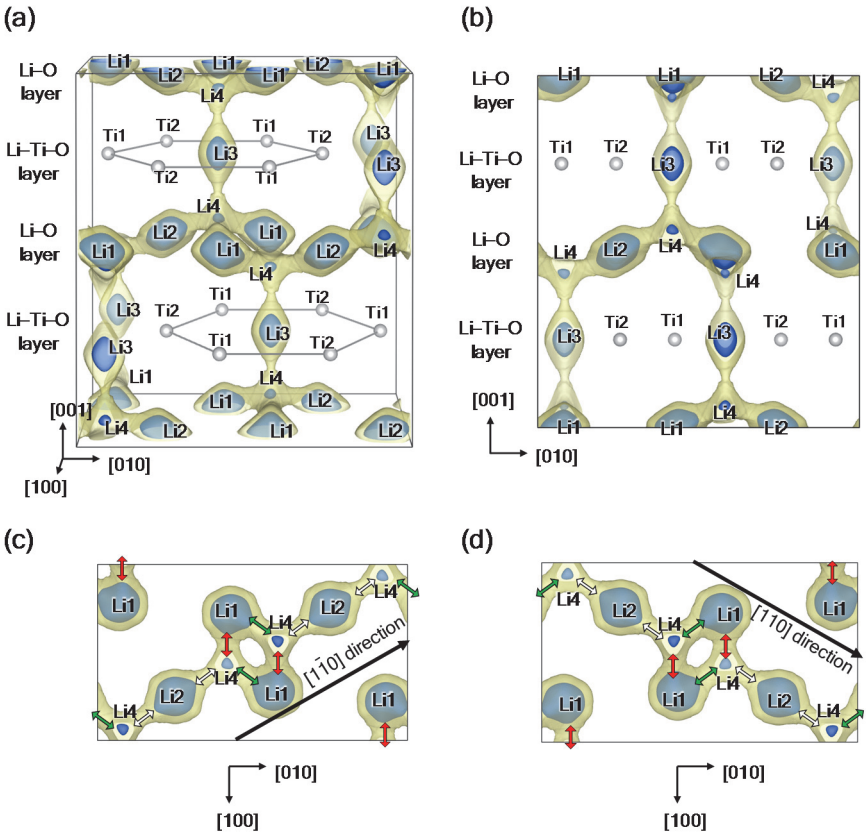

Figure S9. BVS maps in β-Li_2TiO_3, showing the yellow and blue isosurfaces at 1.32 and 1.18 vu, respectively. (a) $0 \le x \le 1$, $0 \le y \le 1$, $0 \le z \le 1$. (b) $-0.05 \le x \le 0.55$, $0 \le y \le 1$, $0 \le z \le 1$). (c) $0 \le x \le 1$, $0 \le y \le 1$, $-0.1 \le z \le 0.1$. (d) $0 \le x \le 1$, $0 \le y \le 1$, $0.4 \le z \le 0.6$. These maps were calculated for the crystal parameters refined using the neutron diffraction data taken with iMATERIA at RT. In panels c and d, the red, green, white and orange arrows denote Li1–Li4, Li1′–Li4, Li2–Li4, and Li3–Li4 paths, respectively.

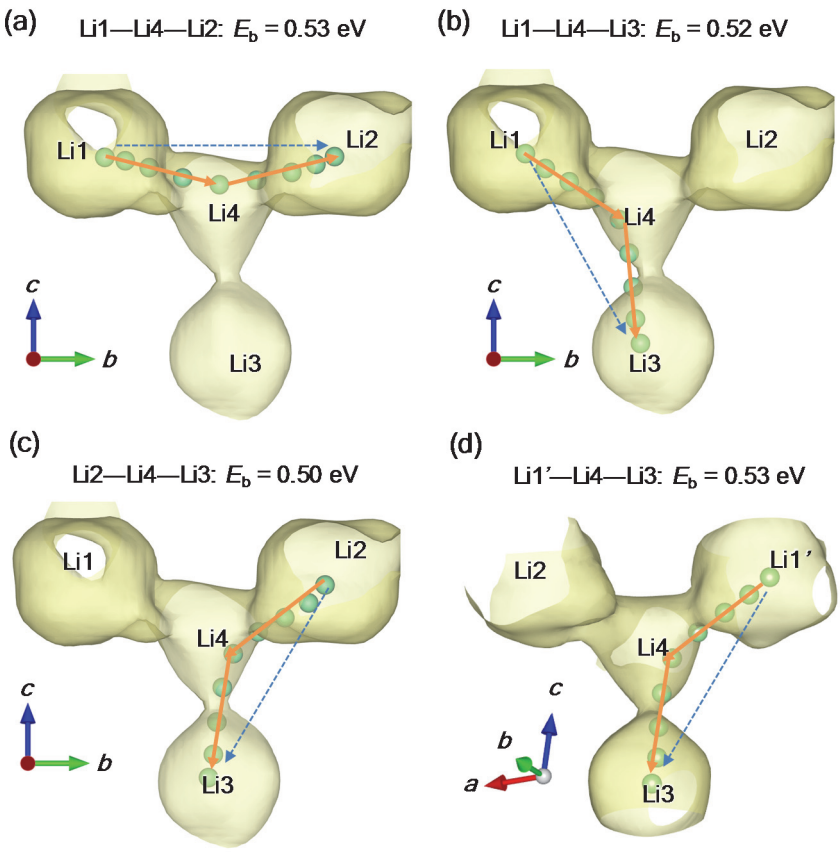

Figure S10. Li-ion migration paths via vacancy mechanism (**a**) –Li1–Li4–Li2–, (**b**) –Li1–Li4–Li3–, (**c**) –Li2–Li4–Li3–, and (**d**) Li1′–Li4–Li3 in β-Li_2TiO_3 calculated using DFT calculations and NEB method, showing the isosurfaces of MEM neutron scattering length densities at –0.04 fm Å^{-3} from the neutron-diffraction data of β-$^7Li_2TiO_3$ at 800 °C. The green spheres represent Li atoms and the blue dashed arrows denote the straight Li-ion migration paths, which directly connect two lattice sites without passing the Li4 site, which do not work. The calculated migration paths (orange lines with arrows) using the NEB method and DFT calculations were consistent with the nuclear-density distribution. The calculated energy barriers for Li-ion migration for (a) –Li1–Li4–Li2–, (b) –Li1–Li4–Li3–, (c) –Li2–Li4–Li3– and (d) Li1′–Li4–Li3 pathways were 0.53, 0.52, 0.50 and 0.53 eV, respectively.

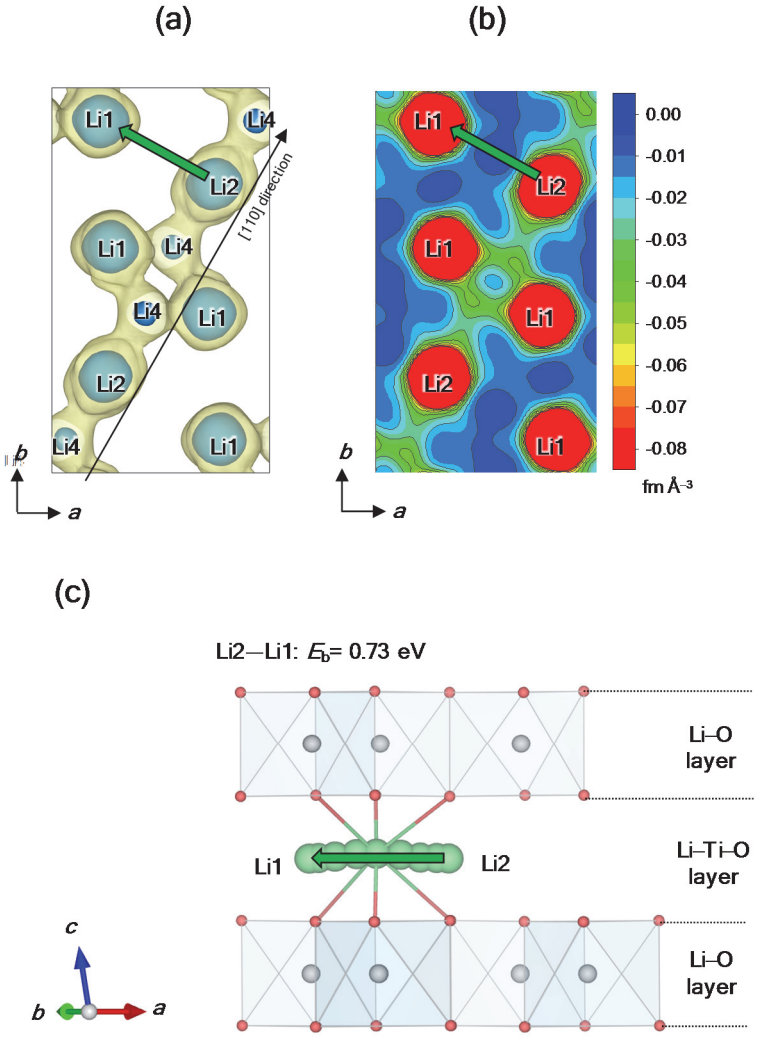

Figure S11. Invalid straight Li-ion diffusion path between Li1 and Li2 sites of β-Li_2TiO_3, which was proposed by Islam et al.[3] (green lines with arrows in panels a, b and c). (a) Yellow and blue isosurfaces of neutron scattering length densities at –0.04 and –0.2 fm Å^{-3}, respectively, which were obtained using the present MEM analysis of neutron-diffraction data of β-$^7Li_2TiO_3$ taken at 800 °C ($0 \le x, y \le 1$, $0.4 \le z \le 0.6$). (b) MEM neutron scattering length density distribution on the *ab* plane at $z = 1/2$ (Contour lines from –0.08 to 0.00 fm Å^{-3} at the interval of 0.01 fm Å^{-3}). Panel c shows the Li-ion diffusion path and migration energy computed by DFT calculations and NEB method (green spheres). The grey and red spheres and blue octahedra represent Ti, O atoms, and TiO_6, respectively. The estimated migration energy for the Li2–Li1 straight path was 0.73 eV, which was much higher than those for the interstitialcy diffusion of Li ion through the interstitial Li4 and lattice Li sites (0.20–0.27 eV) (Figures 5c and 5d).

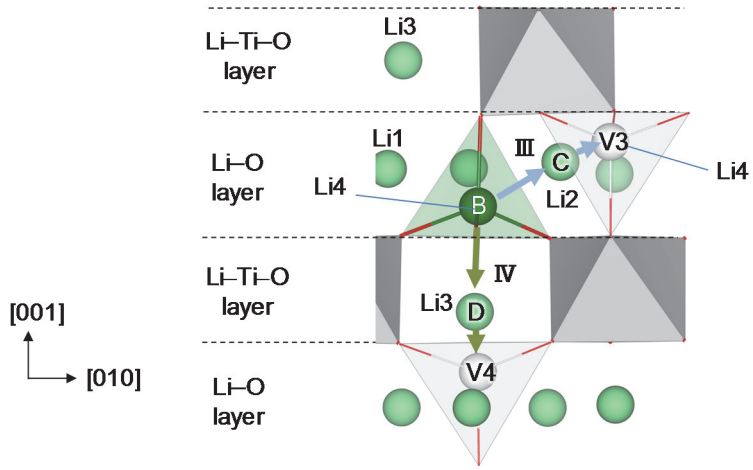

Figure S12. Configurations of Li and Ti atoms for the Bader analysis of β-Li_2TiO_3. B, C, and D represent Li atoms at Li4, Li2, and Li3 sites, respectively. E, F, and G denote neighboring Ti atoms. The calculated Bader charges are listed in Table S7.

Table S7. Bader charges of (a) Li and (b) Ti atoms at the initial state, saddle point, and final state for the Li migration paths III and IV in β-Li_2TiO_3. The migration paths and atom labels are shown in Figure S12. The Bader charge was estimated using the grid-based Bader analysis algorithm after Tang et al.[4]

(a) Bader charge of Li atom remains almost unchanged at +0.87(±0.01), which indicates that the oxidation number of Li cation +1 (Li^+) do not change during its migration.

		Bader charge		
	Li atom label	Initial state	Saddle point	Final state
Path III	B	+0.86	+0.87	+0.88
	C	+0.88	+0.87	+0.86
Path IV	B	+0.86	+0.87	+0.88
	D	+0.88	+0.87	+0.86

(b) Bader charges of the Ti atoms near the paths III and IV. The calculated Bader charges of Ti atoms during the Li-ion migration were equaled to those of the ideal crystal of β-Li_2TiO_3 (Ti1: +2.18 and Ti2: +2.17). The analysis shows no significant change in the Bader charge of neighboring Ti atoms.

		Bader charge		
	Ti atom label	Initial state	Saddle point	Final state
Path III	E	+2.18	+2.18	+2.18
	F	+2.18	+2.17	+2.17
	G	+2.18	+2.18	+2.17
Path IV	E	+2.18	+2.17	+2.18
	F	+2.18	+2.18	+2.18
	G	+2.18	+2.18	+2.18

References

1. Brown, I. D.; Altermatt, D. Bond-valence parameters obtained from a systematic analysis of the inorganic crystal structure database. *Acta Crystallogr. B* **1985**, *41*, 244–247.
2. Cheng, E. J.; Hong, K.; Taylor, N. J.; Choe, H.; Wolfenstine, J.; Sakamoto, J. Mechanical and Physical Properties of $LiNi_{0.33}Mn_{0.33}Co_{0.33}O_2$ (NMC). *J. Eur. Ceram. Soc.* **2017**, *37*, 3213–3217.
3. Islam, M. M.; Bredow, T. Lithium Diffusion Pathways in β-Li_2TiO_3: A Theoretical Study. *J. Phys. Chem. C* **2016**, *120*, 7061–7066.
4. Tang, W.; Sanville, E.; Henkelman G. A grid-based Bader analysis algorithm without lattice bias, *J. Phys.: Condens. Matter* **2009**, *21*, 084204, 1-7.